SCIENCE CHINA
Earth Sciences

• RESEARCH PAPER •

June 2010 Vol.53 No.6: 854–862
doi: 10.1007/s11430-010-0057-4

Advanced characterization of pores and fractures in coals by nuclear magnetic resonance and X-ray computed tomography

YAO YanBin*, LIU DaMeng, CAI YiDong & LI JunQian

School of Energy Resources, China University of Geosciences, Beijing 100083, China

Received October 19, 2009; accepted February 8, 2010; published online April 15, 2010

This paper demonstrates capabilities of low-field nuclear magnetic resonance (NMR) and microfocus X-ray computed tomography (μCT) in advanced, nondestructive, and quantitative characterization of pore types, producible porosity, pore structure, and spatial disposition of pore-fractures in coals. Results show that the NMR transverse relaxation time (T_2) at 0.5–2.5, 20–50, and >100 ms correspond to pores of <0.1 μm, >0.1 μm, and fractures, respectively. A much higher T_2 spectrum peak reflects a much better development of pores (or fractures) corresponding to the T_2, and vice versa. Three basic components in coals, i.e., the pores (or fractures), coal matrix, and minerals have their distinctive range of CT numbers. Among these, the CT number of pores is commonly less than 600 HU. The producible porosity, which is a determination of permeability, can be calculated by T_2 cutoff value (T_{2C}) of coal NMR. The coal pore structure can be efficiently estimated by the newly proposed "T_{2C} based model". Finally, μCT scan was proven capable of modeling and spatial visualization of pores and fractures.

coalbed methane, pore, fracture, nuclear magnetic resonance (NMR), X-ray computed tomography (X-CT)

Citation: Yao Y B, Liu D M, Cai Y D, et al. Advanced characterization of pores and fractures in coals by nuclear magnetic resonance and X-ray computed tomography. Sci China Earth Sci, 2010, 53: 854–862, doi: 10.1007/s11430-010-0057-4

The characterization and evaluation of pores and fractures in coals are important not only for selecting the favorable coalbed methane (CBM) reservoir in exploration but also for designing reservoir engineering parameters during production. Compared to the coal reservoirs in many other regions, those in China are commonly associated with pores and fractures, having low porosity, low permeability, and high heterogeneity. To characterize the coal reservoirs in China, development of new methods is essential that can better quantify pores and fractures to detect coal reservoir characteristics.

Two traditional methods have been commonly used to characterize pores and fractures of coals [1, 2]. One is microscopic observation of coal block, thin slice, or polished slabs using optical microscope or scanning electron microscope (SEM) [3] and the other is the gas adsorption and mercury porosimetry (MIP) [4, 5] for porosity and pore structure analyses. Although these methods have been commercially used, they have some serious limitations. For example, gas adsorption can only obtain information about the micro- and mesopores of coals. For MIP, the elastic compressibility of coal must be considered when high-pressure intrusion by mercury happens [6]. The "columnar capillary pores model" theory used in MIP is sometimes unsuitable for coals [7]. Microscopic techniques (e.g., optical microscope and SEM) can only provide local pictures of a sample. More importantly, all these methods have a common limitation in that they are destructive to the samples, and thus may result in some misleading information on the pores or fractures. In general, all these traditional methods are either destructive to the samples or uninformative for distinguishing pores from fractures in coals. Conse-

*Corresponding author (email: yyb@cugb.edu.cn)

quently, seeking nondestructive techniques such as nuclear magnetic resonance (NMR) and X-ray computed tomography (CT) is important to overcome these deficiencies.

The aim of this study is to demonstrate some advanced, nondestructive, and quantitative methods that can be used to characterize the pores and fractures of coals. In the study, the techniques including low-field nuclear magnetic resonance (LFNMR) [8] and microfocus X-ray computed tomography (μCT) [9] will be discussed. The emphasis of this study is to show the new methods on the quantification of pore types, producible porosity, pore structure, and three-dimensional (3D) visualization of the spatial disposition of pores-fractures in coals.

1 Experimental methods

The coal samples (20 cm×20 cm×10 cm for each) were collected from underground mines of the Ordos basin, the Qinshui basin and the Hongyang coalfield, North China. These samples have vitrinite reflectance (R_o) of 0.39%–5.68%, and include lignite, bituminous, semi-anthracites anthracites and meta-anthracite (Table 1). All coal samples were drilled for cylindrical cores of about 25 mm in diameter. To characterize the pores and fractures of the coals, four sets of experiments were carried out.

Set-I experiment includes porosity and permeability analyses. Prior to the experiment, the coal samples were dried at 80°C for at least 12 h in a vacuum oven. The helium porosity and air permeability were measured using the routine core analysis methods by the Chinese Oil and Gas Industry Standard (SY/T) 5336–1996. The water porosity analysis was performed by a gravimetric method following four procedures. Firstly, the core samples were dried at 80°C for at least 24 h in a vacuum oven. Secondly, bulk volumes and weights were measured, and dry densities of the samples were calculated. Thirdly, these samples were dried for 8 h in a vacuum oven, and then they were saturated with 100% distilled water for at least another 24 h. Finally, bulk volumes and weights were remeasured, and wet densities were calculated. The water porosities of the samples were calculated by the values of dry densities and wet densities.

Set-II experiment includes two sets of NMR measurements. Prior to the experiment, the coal samples were prepared by the following procedure: 1) they were dried at 70°C for 24 h in a vacuum oven; 2) they were vacuumed for 8 h; and 3) they were saturated in 100% distilled water for 8 h. After the experimental preparation had been finished, two sets of NMR measurements were performed. Firstly, the NMR measurement at 100% water-saturated condition (S_w) was performed for all samples. Secondly, a centrifuged experiment was arranged to obtain a perfect irreducible water conditions (S_{ir}) for nine selected samples. The used centrifuge pressure and time are 200 Psi and 1.5 h, respectively. Finally, the NMR measurement at S_{ir} was performed for the nine samples. As a result, NMR measurements obtained two transverse relaxation time (T_2) spectra: one at S_w and another at S_{ir}. The T_2 spectra can be used to study the pores and fractures of coals.

The NMR measurements used a Rec Core 2500 instrument with a resonance frequency of 2.38 MHz. The detailed discussion about the instrument, the experiment elements, and the experiment procedures were reported elsewhere [8]. It should be noted that the NMR measurement parameters of coals are different from those of sandstones due to their different pore structures. Thus, NMR measurement parameters including the echo spacing (T_E) and the waiting time (T_W) need to be carefully considered before the experiment. As an important result of NMR measurement, the configuration of relaxation time distribution varies with the parameters of T_E and T_W. For a given T_W, the T_2 spectra distribution would move to the right with increasing T_E. Thus, the T_E should be set as small as possible; otherwise some information of micropores would be omitted. For a given T_E, the T_W should be as higher as possible; otherwise some pore information would be omitted. In this study, the main NMR measurement parameter sets include the T_E of 0.6 ms, the T_W of 5 s, the echo numbers of 2048, the scanning numbers of 64, and the environment temperature of 25°C.

Table 1 Sampling locations, coal seams and vitrinite reflectances of the selected coal samples

Sample No.	Coalfield/Basin	Coal mine	Age	Coal seam	R_o (%)
1	Ordos Basin	Hongce	Jurassic	$3^{\#}$	0.39
3		Wulan	Carboniferous	$7^{\#}$	1.01
4		Shitanjing-1	Carboniferous	$10^{\#}$	1.56
2	Hongyang Coalfield	Linsheng	Permian	$5^{\#}$	0.8
9		Xima	Carboniferous	$12^{\#}$	2.7
10		Hongling	Carboniferous	$12^{\#}$	2.7
5	Qinshui Basin	Yangquan-2	Carboniferous	$15^{\#}$	1.87
6		Yangquan-1	Permian	$3^{\#}$	2.15
7		Yangquan-3	Permian	$3^{\#}$	2.38
8		Shihe	Permian	$3^{\#}$	2.42
11		Changzhen	Permian	$3^{\#}$	3.57

Set-III experiment is the μCT analysis. The experiment was performed on an ACTIS-225FFI CT/DR/RTR microfocus CT scan equipment manufactured by BIR Corporation of USA. During operation, the spatial resolution is approximately 70 μm, with which most pores and all fractures can be distinguished. The detailed discussion about the experiment including the measuring parameters, method, and procedures were reported elsewhere [9].

Set-IV experiment is the MIP. The purpose of this experiment is to verify the results of NMR measurement. Seven samples were selected for the MIP by the SY/T 5346–2005. Mercury intrusion/withdrawal curves were measured and used to generate the pore size distributions.

2 Pores types and morphology

2.1 Pores types

LFNMR means the NMR measurement in condition of a very low external magnetic field. In the low magnetic field, the number of hydrogen atoms present within the fluid of a rock can be detected by means of a relationship between T_2 distribution (also called T_2 spectrum) and relaxation time, and thus the physical properties of the rock and seepage characteristics of fluid in the rock can be analyzed [10]. Since the 1980s, this method has become an indispensable tool for characterizing properties of reservoir rocks such as sandstones and carbonates [11–15]. However, nearly no research has been conducted on the petrophysical analysis of coals using this method.

The application of LFNMR in studying pore types of coals is based on the fact that the relaxation time of hydrogen atoms present within pores is positively correlated to the pore size. Consequently, a T_2 distribution corresponds to a pore size distribution with the smallest pores having the shortest relaxation times and the largest pores having the longest relaxation times.

There are three reasons for the fact that LFNMR can be used for coals. Firstly, the application element of LFNMR on coals is similar to that on sandstones. Secondly, coal is a kind of weak magnetic substance. In the very low field condition, a few paramagnetic minerals within coals cannot influence the measured results. Finally, in the very low resonance frequency, the magnetic information of solid state proton (^{13}C and ^{1}H) can be shielded, thus they cannot influence the measured results by LFNMR [8].

The pore types of coals include the micropores (<0.1 μm), the macropores (>0.1 μm), and fractures. It is found that in a typical T_2 spectrum, from short to long relaxation times, the micropores, macropores, and fractures can be identified. On the one hand, based on the comparison of T_2 spectra at S_w and S_{ir}, the micropores can be distinguished from the macropores, because according to the Washburn equation, the centrifuging pressure of 200 Psi corresponds to the pore size of 0.1 μm [8]. In other words, the T_2 spectrum at S_w represents information of all pores, while the T_2 spectrum at S_{ir} only represents information of all micropores and some macropores. On the other hand, the macropores and the fractures can be differentiated by their respective T_2 spectrum peaks. In the T_2 spectrum of sample 9 (Figure 1), for example, three peaks correspond to the micropores, macropores, and fractures, respectively. The micropores are associated with the spectrum peak located at 0.5–2.5 ms. The micropore peak is always coincident before and after the centrifuge experiment. The macropores associated with the spectrum peak are located at 20–50 ms. The macropore peak is commonly lower than the micropore peak. It is observed that some parts of the macropore peak have been weakened through the centrifuge experiment. The fracture is associated with the spectrum peak located at >1000 ms. The fracture peak can only be found in a T_2 spectrum of S_w, but not in the T_2 spectrum of S_{ir}. Based on the statistics of the selected samples, the pore type found in coals is mostly the micropores, and then the macropores. The fracture was only found in a few samples. Additionally, the anthracites are commonly developed with extremely high proportion of the micropores in their pore types.

It is also found that the T_2 distribution characteristics including the number, size, and position of T_2 spectrum peaks, can be used to analyze pore types of coals. For example, for the three T_2 spectrum peaks of sample 9 (Figure 1), the micropore peak is the biggest, meaning that the micropores are well developed. There is scarcely any difference between the T_2 spectra at S_w and the T_2 spectra at S_{ir}. This means that the poor-connectivity between micropores and macropores has held back the water on the surface of micropores to be centrifuged. The macropore peak is small, meaning that the macropores are not very well developed. At the same time, the macropore peak was weakened by centrifuging, meaning that the moderate-connectivity of macropores induced the discharge of some free water. Comparably, the fracture peak totally disappeared after the centrifuge, which is a typical indication of the well-connectivity of fractures. Additionally, the poor continuity between the micropore and macropore peaks represents the poor connectivity between micropores and macropores, whereas the good continuity between the macropore and fracture peaks represents the good connectivity between macropores and fractures.

Furthermore, it seems that the fully saturated T_2 distributions depend on coal ranks. As shown in Figure 2, with increasing coal rank the T_2 distribution of samples 1–9 show various pore characteristics. Sample 1, a sub-bituminous coal, is developed with dominating micropores, a few fractures, and minor macropores. Sample 2, a high volatile bituminous coal (HvB), contains mainly macropores and fractures. Sample 3, a medium volatile bituminous coal (MvB), is characterized with dominating fractures and a few micropores and mesopores. Sample 4, a low volatile bituminous coal (LvB), has mostly macropores and micropores,

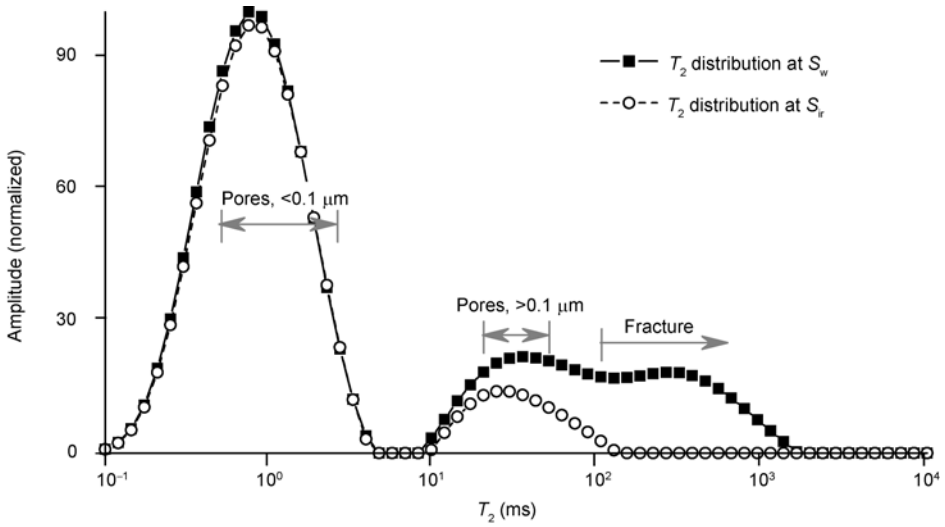

Figure 1 Typical T_2 distributions showing the developments of pores and fractures in No. 9 sample.

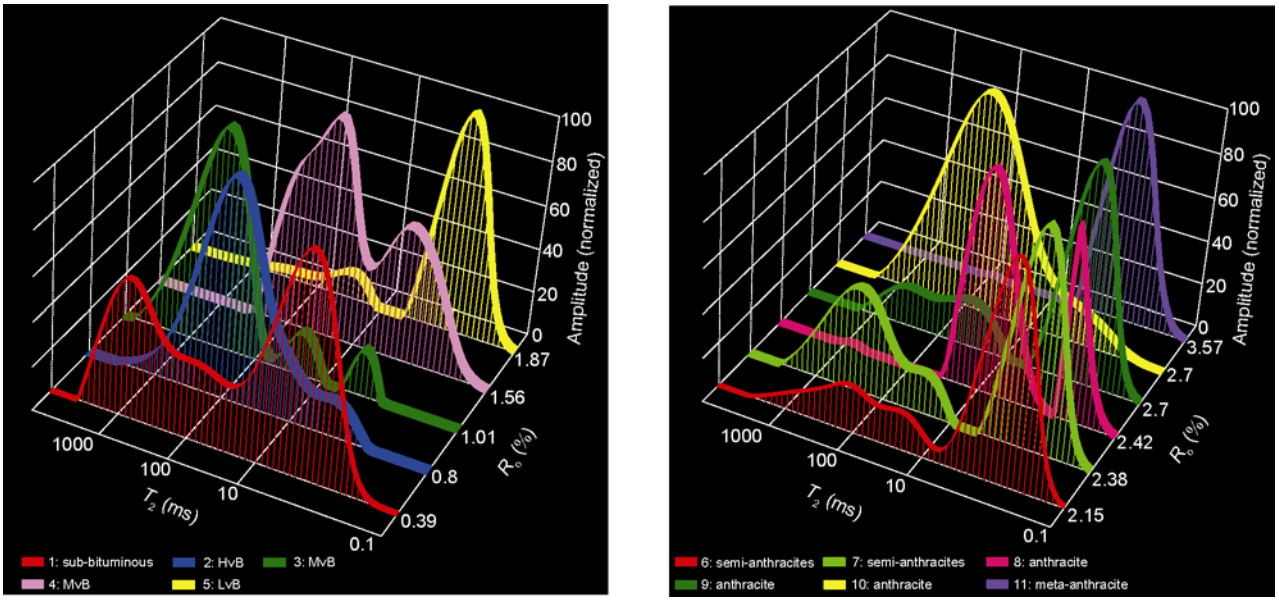

Figure 2 NMR T_2 distributions of bituminous coals and anthracites (100% water saturated condition). 1–11, sample No.

but few fractures. Samples 5–11 are anthracites. They have dominating micoropores with typical T_2 spectrum peaks at 0.5–2.5 ms. Sample 10, a special anthracite was collected adjacent to a dike. Different from samples 5–11, sample 10 has well-developed macropores and fractures but minor micropores. This is because that the magma contact metamorphism may have resulted in change of the pore structure, leading to the formation of groups of gaspores (belonging to macropores) [9]. In general, with increasing coal rank it was found that 1) from the sub-bituminous to MvB, there is a decrease in micropores and an increase in macropores; 2) in the metamorphism region of LvB coal, micropores decrease rapidly; and 3) in the metamorphism region of anthracite, pores in coals are mostly micropores. The effects of coal rank upon T_2 distribution are possibly due to the structure changes resulting from pore structure changes during coalification.

2.2 Pores morphology characteristics by μCT

Advanced characterization of pores and fractures of coals can be implemented by the μCT, which has been reported in a few papers [9, 16–18]. Theoretically, in CT scanning, as X-rays passes through the coal being scanned, the signal is attenuated by scattering and absorption. The linear attenuation is a function of both density and effective atomic number of the coal, and it can be represented by the CT number. The CT number distribution among the scanned coal shows

the detailed information of coal microstructure. In this study, it is considered that the physical microstructure of the coal is composed of the organic components, inorganic minerals, and the void space including inner pores, cleats, and other fractures. Since the three basic components are different in both effective atomic number and density, their CT numbers are also different. Based on the discrepancy of CT numbers, pores, fractures, and minerals can be distinguished [9].

A total of 11 samples were selected for μCT analyses. Along its axial direction, every sample was scanned 80 times to obtain 80 consecutive gray images. These gray images are used to reconstruct 3D data of the sample. For example, the 3D reconstruction of sample 10 is shown in Figure 3. Figure 3(a)–(c) shows the image-slices in the posterior (P)-anterior (A) direction, the top (T)-bottom (B) direction, and the right (R)-left (L), respectively. Figure 3(d) shows the CT numbers distribution along the profile line in Figure 3(b). In a typical binary black-white image, each pixel corresponds to a grayscale that is correlated with a CT number: 1) void space with low CT number corresponds to the black; 2) minerals with high CT number correspond to the white; and 3) organic components with medium CT number correspond to the gray color. Although for coals with different coal rank or different coal composition (organic or inorganic) the variation of CT number may be different, it was found that the CT numbers of minerals, coal matrix, and pores (including fractures) are stable at approximately 3000 HU, 1000–1800 HU, and <600 HU, respectively. For example, batches of gas pores resulted from the magma contact metamorphism are observed in sample 10. Fractures are also well developed, and some parts of them are found to be filled with minerals. As shown in Figure 3(d), the CT number profile line cross two pores and one fracture, where the CT numbers get three minima (<300 HU): the higher porosity obtains the lower CT number. The CT number profile line crosses the area of two minerals, where the CT numbers get two maxima (about 3000 HU). Along the profile line, the CT numbers of coal matrix (including all coal maceral composition) are commonly located at 500–1000 HU. Based on Figure 3(a)–(c), it is found that 1) two sets of fractures are well developed as orthogonal to each other, with a set of dominating fracture in axial direction; 2) these fractures are partially filled with some lamellar minerals; 3) the rounded gas pores are well developed with the size of about 0.1–1 mm, and they are organized as banded assemblages along the fracture directions; and 4) the well developed pores and fractures result in a gas permeability of 14.9 mD for this coal. In general, it is concluded that the μCT method can be applied for advanced characterization of the morphology, size, and the 3D spatial disposition of the minerals, pores, and fractures in coals.

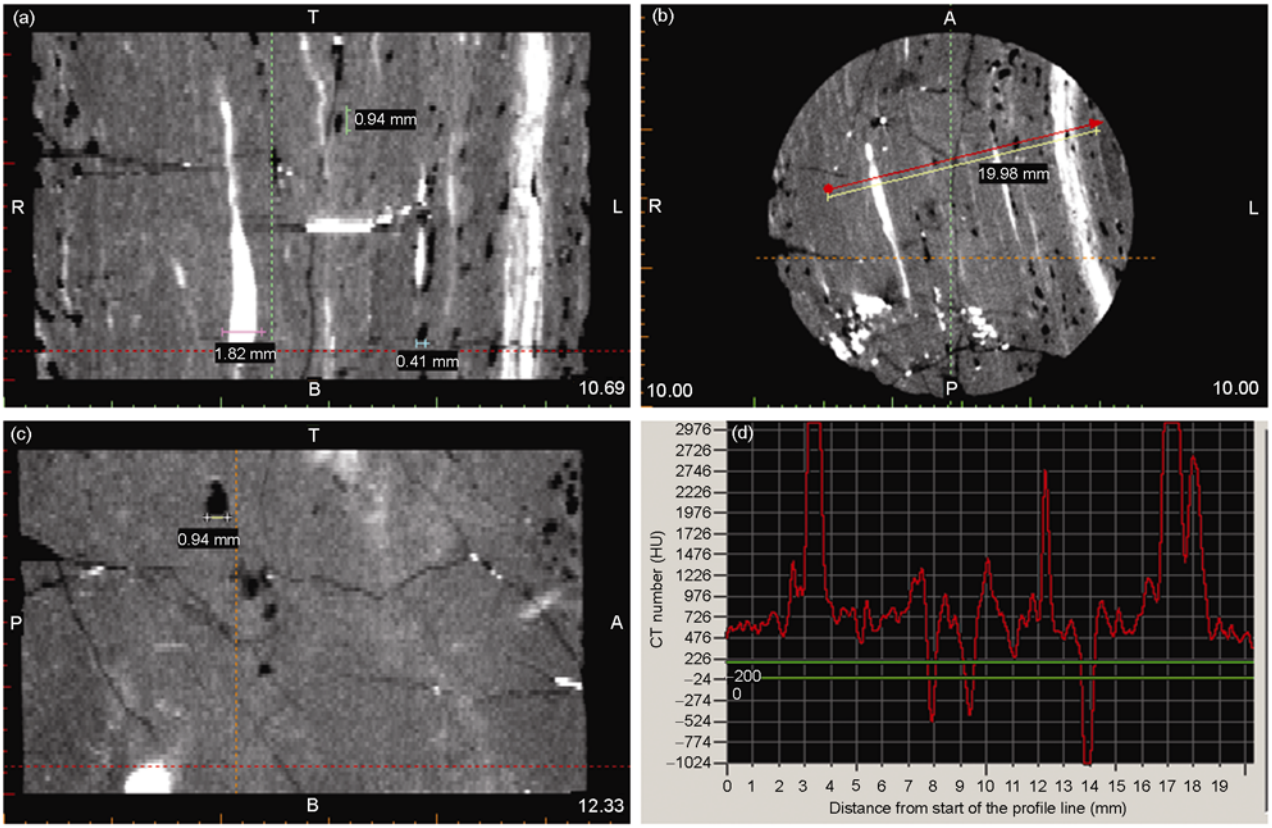

Figure 3 CAD 3D-view showing pores (black spot), fractures (black line) and minerals (light white area) in coals and their CT numbers (No. 10 sample). (a) Posterior (P)-anterior (A) direction; (b) top (T)-bottom (B) direction; (c) right (R)-left (L) direction; (d) CT number distribution along the profile line in (b).

3 Porosity

3.1 Total porosity

CBM reservoir is a typical low-porosity and low-permeability reservoir. In CBM reservoir, methane flows through the pore and fracture network to the wellbore. Consequently, much of permeability is accounted for how well the pore and fractures develop. Generally, evaluation of the development of pore and fracture is related to the total porosity. Total porosity (also called porosity) is defined as the pore volume percentage occupied by pores. It includes not only the connective (producible) porosity but also the close (irreducible) porosity. In this study, the helium gas method, water saturation method, and MIP were used to measure the porosity. The results show that except sample 1, which was broken and failed for measurement under saturation, all coals have very little difference between the MIP porosity (φ_{MIP}) and water-saturated porosity (φ_w). The φ_{MIP} and φ_w are of 1%–5%. The porosity by helium method (φ_g) ranges from 1.56% to 9%, higher than those from the other two methods by an average extension of 1%–2%.

The φ_g vs. φ_w shows a strong positive linear correlation:

$$\varphi_g=1.19\varphi_w+0.76, \quad (1)$$

where the goodness-of-fit is about 0.84. The linear slop of 1.19 means that for the same sample, φ_g is higher than φ_w with an average extension of 1.19%. The reason for this extension is that the gas can access more micropores than the water.

3.2 Producible porosity

The producible porosity is the pore volume percentage occupied by connective pores. It contributes mostly to gas permeability, and thus it has become an important parameter for evaluating CBM reservoir. As discussed earlier, although many traditional methods have been commercially used to analyze coal porosity, there are few methods to analyze the producible porosity. In this study, we found that the producible porosity could be calculated by combining these traditional methods and the LFNMR.

In order to obtain the producible porosity, two sets of T_2 distribution measurements were performed. Firstly, the NMR measurement at S_w was performed, and an incremental T_2 spectrum was obtained (Figure 4). The incremental T_2 spectrum was then transformed into an accumulative T_2 spectrum. In the accumulative T_2 spectrum, the longitudinal axis of the spectrum represents relaxation amplitude of ^{1}H at different time. Since the relaxation amplitude is a dimensionless variable, the accumulative relaxation amplitude is formatted to be equal to total porosity [8, 10]. Secondly, the NMR measurement at S_{ir} was performed, and an incremental T_2 spectrum was obtained. The incremental T_2 spectrum was also transformed into an accumulative T_2 spectrum. In the accumulative T_2 spectrum of S_{ir}, the accumulative relaxation amplitude is formatted to be equal to the irreducible porosity. As a result, the difference between the producible porosity and total porosity is the producible porosity. For example, in sample 4, the water-saturated porosity of the sample (0.85%) was assigned to be the total porosity and then the irreducible- and producible porosities were calculated as 0.36% and 0.49%, respectively (Table 2).

In this study the producible porosity was calculated for 9 samples. The result shows that the producible and irreducible porosities are different from sample to sample. The correlation between them is poor: some samples with high total porosities may have low producible porosities, and *vice versa* (Table 2). It is also found that the permeability is strongly correlated to the producible porosity, but not the irreducible porosity. This result shows the significance of partitioning the producible from irreducible porosities by LFNMR method.

As discussed above, the pore type can be distinguished by the T_2 distribution. Thus, it is certain that in a T_2 spectrum, there is a T_2 cutoff value (T_{2C}) that divides the T_2

Table 2 Porosities and permeability of selected samples

Sample No.	Permeability (mD)	Total porosity (%)			Irreducible porosity (%)	Producible porosity (%)
		φ_w	φ_g	φ_{MIP}		
1	82.1	–	6.7	13.5	–	–
2	0.002	1.41	2.27	1.4	1.14	0.27
3	3.09	3.21	5.2	–	0.45	2.76
4	0.067	0.85	2.3	–	0.36	0.49
5	0.012	3.97	4.3	4.0	3.63	0.34
6	0.094	3.26	5.8	3.3	–	–
7	0.0044	1.74	3.01	1.7	1.03	0.71
8	0.009	2.42	3.12	2.4	2.3	0.12
9	1.2	5.09	5.43	5.1	3.92	1.17
10	14.9	5.88	9	–	1.21	4.67
11	0.00032	1.03	1.56	–	0.96	0.07

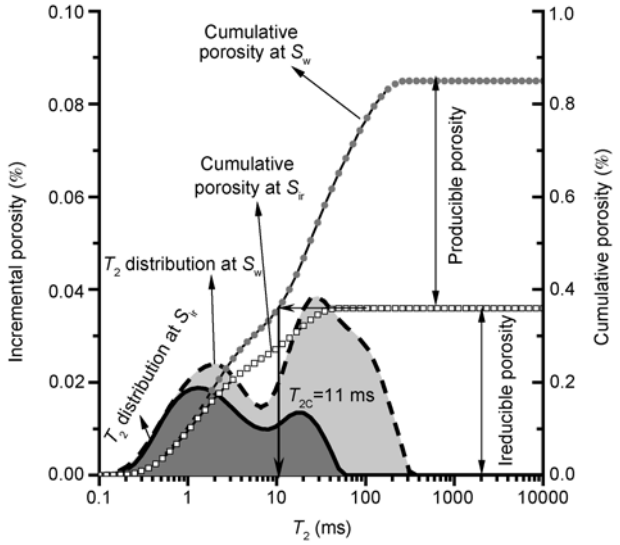

Figure 4 Irreducible and producible porosities, showing the method to calculate a T_{2C}.

spectrum into two parts: the irreducible water and the free water. The irreducible water in pores has characteristics of $T_2<T_{2C}$, whereas free water in pores with characteristics of $T_2>T_{2C}$ is treated as movable or producible [10]. In fact, T_{2C} is also the threshold between irreducible and producible porosities. As shown in Figure 4, for a coal with certain total porosity, its T_2 spectrum would move left with increasing producible porosity. This means that on the one hand, the high producible porosity commonly has a low T_{2C} and on the other hand, the producible porosity is determined by both the total porosity and the T_{2C}.

Since the T_{2C} is important to the producible porosity, it commonly needs to be estimated. Figure 4 shows the process for determining T_{2C}. Firstly, both the accumulative porosity curve at S_w and the accumulative porosity curve at S_{ir} need to be done. Secondly, a horizontal projection from the cumulative curve at S_{ir} needs to be done. Finally, vertical projection from the cumulative curve at S_w needs to be done. The T_2 value at the intersection projected on the T_2 axis is the T_{2C}. The calculated T_{2C} of sample 4 is 11 ms. Moreover, T_{2C} is also important for the evaluation of pore structure, which will be discussed below.

4 Pore structure

The pore structure (pore size distribution) is also important for CBM seepage. Poor pore structure may lower the gas permeability by the "bottle neck" effect [1]. As discussed before [4, 5], coal pore structure was evaluated by combining the gas adsorption method and MIP. The pore size distribution histogram by MIP shows high coincidence with T_2 distribution [8]: a high proportion of micropores by MIP corresponds to a distinct T_2 spectrum peak of micropores, while a high proportion of macropores by MIP corresponds to a distinct T_2 spectrum peak of macropores.

Previous studies have proposed many transform methods to obtain the pore structure from NMR data. These methods are proven suitable for sandstone [10, 19, 20]; however, they are proven unfitted for the coals used in this study because the methods are hard to use [8]. Therefore, a new method, also called "T_{2C} based model", has been proposed for scaling the NMR pore structure. The method is based on the principle that any relaxation time in the T_2 distribution corresponds to a certain pore size of the coal sample: slow relaxation times correspond to larger pores and *vice versa*. To quantify the relationship between relaxation time and pore size, a key parameter of T_{2C} is used. Since T_{2C} was determined by a centrifuge experiment and two NMR experiments, the certain pore size (r) corresponding to the certain T_{2C} value can be determined. For any relaxation time (T_{2i}) in a T_2 relaxation distribution, the corresponding pore size (r_{ci}) can be determined by eq. (2).

$$r_{ci} = r\, T_{2i} / T_{2C}. \quad (2)$$

As discussed in section 2.1, r is about 0.1 μm in this study. Based on eq. (2), the pore size distribution by NMR data is determined.

The pore size distributions by MIP and the results by "T_{2C} based model" are shown in Table 3. The constructive pore

Table 3 Comparison of pore size distributions by MIP and by "T_{2C} based model"

Sample No.	Method	Pore size distribution (vol.%)				
		<0.1 μm	0.1–0.25 μm	0.25–0.64 μm	0.64–1 μm	>1 μm
2	MIP	61.17	12.09	7.64	3.10	16.00
	NMR	79.22	14.61	4.93	0.95	0.29
5	MIP	88.60	2.44	1.00	0.43	7.53
	NMR	90.95	4.25	2.09	1.04	1.67
7	MIP	54.41	5.67	5.17	3.51	31.24
	NMR	57.99	6.58	9.61	5.22	20.60
8	MIP	83.63	4.08	1.59	0.62	10.09
	NMR	94.41	4.89	0.00	0.00	0.70
9	MIP	83.07	3.18	2.63	1.77	9.35
	NMR	78.37	5.69	6.07	2.54	7.33

size distributions coincide very well with the pore size distributions estimated from MIP, meaning that the pore structure estimated by NMR is reliable. From further comparison of the two pore structures, it was found that the pore structure estimation on miropores (<0.1 μm) is more accurate than that on macropores pores (>0.1 μm). Moreover, the estimated percentages of extra-macropores (>1 μm) are distinctly lower than the measured results by MIP. The reason is induced by the MIP itself. The MIP has a drawback in coal characterization because of the compressibility of coal [6]. The MIP is based on Washburn equation: increasing pressure makes smaller pores accessible to mercury [7]. At the early intrusion phase with lower mercury pressure, mercury abruptly intrudes into the pores and intrusion volume increases rapidly. At this phase, the pressure and intrusion volume do not match well with the Washburn equation. This phenomenon commonly results in overestimations of intrusion volume and the proportion of macropores [6, 7]. Comparably, as a nondestructive method, LFNMR does not overestimate the macropore proportion. In general, although the pore size distribution of coal can be evaluated by the LFNMR method, the accuracy of this method could still be improved.

5 Spatial dispositions of pores and fractures

Pores and fractures are highly heterogeneous in 3D reservoir, and the main fracture is commonly developed in a dominating direction. The accurate determination of the fracture direction is important for designing CBM well. By using the μCT, the size and the direction of fractures not only can be nondestructive and qualitatively evaluated, but also can be visualized in 3D. This is a particular advantage of μCT method.

To study the spatial distribution of pores, fractures, and minerals, 3D visualization of coal samples was conducted. The 3D visualization is based on the fact that coal matrix, pores (including fractures), and minerals have their respective CT number intervals. Consequently, in a 3D coordinate set, they can be modeled and visualized. There are three models commonly used in the visualization: the 3D-surface and 3D-volume rendering models, and the computer-aided design (CAD) model. The results of surface and volume rendering models are 3D representations of the surface and volume of the coal. Here the applications of the two models on characterization of coal will be shown.

Figure 5 shows the surface and volume renderings for visualization of No.1 coal. In this figure, the organic component, and void space (e.g., pores and cleats) are set as transparent and orange, respectively. The minerals are set as black in Figure 5(a) and brown in Figure 5(b). A face cleat and butt cleat system with good connectivity is clearly identified in both figures. The face cleat is developed in the axial direction, and it is vertical to the butt cleat. The cleat space is commonly <2.5 mm. A few groups of pores are developed around the cleats. Some nodule-like minerals are distributed among the coal. In general, the coal has well-connected and non-mineralized cleats, which is the reason of the high permeability (82.1 mD) of the coal.

It is still in the primary stage in using μCT to quantify the spatial distribution of pores, cleat, and minerals. It would be very promising to use this technique to characterize the coal heterogeneity, to dynamically simulate the transform of fluid, and to evaluate porosity and permeability change due to the pressure change when recovering CBM. It would be very meaningful to extend these studies in the future.

6 Conclusions

Based on the experiments of 11 coal samples with various coal ranks, LFNMR and μCT are proven to be useful for advanced characterization of pores and fractures of coals. LFNMR has advantages in differentiating irreducible and producible porosities, and in quantifying coal pore structure, whereas μCT has advantages in 3D characterization of pores and fractures. By combing the two methods, the pore type, producible porosity, pore structure, and spatial disposition

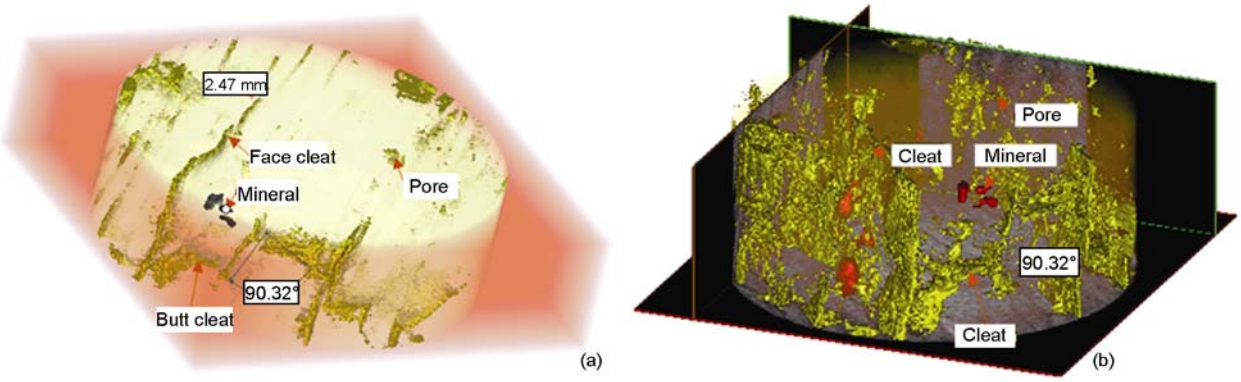

Figure 5 3D surface (a) and volume (b) renderings for visualization of sample 1.

of pore-fractures in coals can be nondestructively and quantitatively characterized.

(1) In a typical NMR T_2 distribution of coals, the T_2 spectrum peaks at 0.5–2.5, 20–50 and >100 ms correspond to micropores (<0.1 μm), macropores (>0.1 μm) and fractures, respectively. In a typical T_2 spectrum of anthracites the micropore peak can be distinctly identified, which is different from bituminous coals.

(2) Three basic components in coals, i.e., the pores (including fractures), coal matrix, and minerals, have their respective CT number ranges of <300 HU, 1000–1800 HU, and 3000 HU, respectively. This is why the μCT can be used for advanced evaluation of pores, fractures, and minerals in coals.

(3) Based on a certain T_{2C} value, coal porosity can be divided into the irreducible and producible porosities, and the latter is a determination of permeability.

(4) Based on the NMR T_2 distribution, a "T_{2C} based model" method was proposed. This method is efficient for estimating the coal pore structure.

(5) Three-dimensional characterization of coal was achieved by the μCT method. The method is capable of analyzing pore size, pore morphology and 3D spatial disposition of pores, fractures, and minerals in coals.

We especially thank Dr. Ganqing Jiang in University of Nevada at Las Vegas for his help in improving the manuscript. This study was supported by National Major Research Program for Science and Technology of China (Grant Nos. 2008ZX05034-01 and 2008ZX05062-001), National Basic Research Program of China (Grant No. 2009CB219604), National Natural Science Foundation of China (Grant No. 40972107), PetroChina Innovation Foundation (Grant No. 2008D-5006-01-04), and Program for Changjiang Scholars and Innovative Research Team in University (Grant No. IRT0864).

1 Yao Y B, Liu D M, Tang D Z, et al. Reserving and recovering characteristics of coalbed methane in coal reservoirs in North China (in Chinese). Petro Exp Dev, 2007, 34: 664–668
2 Sing K S W. Characterization of porous materials: Past, present and future. Colloid Surface A, 2004, 241: 3–7
3 Yao Y B, Liu D M, Huang W H, et al. Research on the pore–fractures system properties of coalbed methane reservoirs and recovery of coalbed methane in Huainan and Huaibei coal-fields (in Chinese). J China Coal Soc, 2006, 31: 163–168
4 Yao Y B, Liu D M, Tang D Z, et al. Fractal characterization of adsorption-pores of coals from North China: An investigation on CH_4 adsorption capacity of coals. Int J Coal Geol, 2008, 73: 27–42
5 Yao Y B, Liu D M, Tang D Z, et al. Fractal characterization of seepage-pores of coals from China: An investigation on permeability of coals. Comput Geosci, 2009, 35:1159–1166
6 Suuberg E M, Deevi S C, Yun Y. Elastic behaviour of coals studied by mercury porosimetry. Fuel, 1995, 74: 1522–1530
7 Gane P A C, Ridgway C J, Lehtinen E, et al. Comparison of NMR cryoporometry, mercury intrusion porosimetry, and DSC thermoporosimetry in characterizing pore size distributions of compressed finely ground calcium carbonate structures. Ind Eng Chem Res, 2004, 43: 7920–7927
8 Yao Y B, Liu D M, Che Y, et al. Petrophysical characterization of coals by low-field nuclear magnetic resonance (NMR). Fuel, 2009, doi: 10.1016/j.fuel.2009.11.005
9 Yao Y B, Liu D M, Che Y, et al. Non-destructive characterization of coal samples from China using microfocus X-ray computed tomography. Int J Coal Geol, 2009, 80: 113–123
10 Coates G R, Xiao L Z, Prammer M G. NMR Logging Principles and Applications. Houston (Texas): Gulf Publishing Company, 1999. 1–76
11 Kevin M, Douglas M, Smith A. NMR technique for the analysis of pore structure: numerical inversion of relaxation measurements. J Colloid Interface Sci, 1987, 19: 117–126
12 Hodgkins M A, Howard J J. Application of NMR logging to reservoir characterization of low-resistivity sands in the gulf of Mexico. AAPG Bull, 1999, 83: 114–127
13 Wang W M, Sun D Q, Miao S, et al. The fundamental study on NMR logging (in Chinese). Well Log Tech, 1997, 21: 385–392
14 Wang X W, Xiao L Z, Xie R H, et al. Study of NMR porosity for terrestrial formation in China. Sci China Ser G-Phys, Mech Astron, 2006, 49: 313–320
15 Kenyon W E. Nuclear magnetic resonance as a petrophysical measurement. Nucl Geophys, 1992, 6:153–171
16 Karacan C Ö, Okandan E. Fracture/cleat analysis of coals from Zonguldak Basin (northwestern Turkey) relative to the potential of coalbed methane production. Int J Coal Geol, 2000, 44: 109–125
17 Van Geet M, Swennen R. Quantitative 3D-fracture analysis by means of microfocus X-ray computer tomography (μCT): An example from coal. Geophys Res Lett, 2001, 28: 3333–3336
18 Mazumder S, Wolf K H A A, Elewaut K, et al. Application of X-ray computed tomography for analyzing cleat spacing and cleat aperture in coal samples. Int J Coal Geol, 2006, 68: 205–222
19 Yakov V. A practical approach to obtain primary drainage capillary pressure curves from NMR core and log data. Petrophysics, 2001, 42: 334–343
20 Liu T Y, Xiao L Z, Fu R S, et al. Applications and characterization of NMR relation derived from sphere capillary model (in Chinese). Chin J Geophys, 2004, 47:663–671